Verification of upconversion in ZBLAN:Ho^{3+} glass under photon-avalanche-type excitation at 980 nm

P. Stremplewski · C. Koepke · D. Piątkowski

Abstract Following earlier predictions, we have attempted to excite a Ho^{3+}:ZBLAN sample into the absorption-less region (980 nm) and obtained a distinct upconverted emission at ∼540 nm accompanied by two other longer wavelength bands. After performing additional lifetime measurements and simulation of the system kinetics, we provide a simple interpretation of the obtained results.

1 Introduction

ZBLAN glass activated by Ho^{3+} ions is a well-known material exploited in numerous papers [1–5]. However, this material, of promising optoelectronic applications [6], is usually being excited into those spectral regions that coincide with maxima of the ground state absorption (GSA) and provide a concrete effect, e.g. optical gain at around 1200 nm or other emission bands potentially attractive in various applications. The very rare cases of excitation into the practically absorption-less region are mostly connected with photon avalanche (PA) research [2, 7]. It is an interesting problem itself: where does the first excited ion come from in such a kind of multiplying excitation? Of course, as mentioned in [7], the absorption band tail can do the trick (it is there identified as the non-resonant phonon sideband GSA). To fulfill the conditions required for starting a full PA cycle, one additionally needs to reach an excitation power threshold [7]. In our case only the first condition of PA is satisfied, i.e. non-resonant pumping and only in this context we use 'photon-avalanche-type' in the title. For the excitation a

980-nm line of a semiconductor laser was used. This kind of excitation, being evidently non-resonant, can be connected with 'borrowing' phonons from the lattice [8, 9] to end up with the excitation in the $^5I_5$ state [10]. As shown later, supported by the kinetic analysis, the observed upconverted emissions can be explained even in the frame of a single ion, without energy transfer. However, in the face of 2.5 mol% concentration, as used in this work, the ion–ion energy transfer is an inherent feature of the de-excitation process; hence, we include the ion–ion energy transfer in our kinetic analysis. Unlike in the case of glasses co-doped with Yb^{3+} and Ho^{3+}, where upconverted emission appears due to the energy transfer between Yb^{3+} and Ho^{3+} ions [11], the crucial mechanism providing higher energy state occupation is the excited state absorption (ESA).

2 Experimental

The examined samples were developed and produced by Fiber Labs Co., Japan, and the composition of ZBLAN glass is rather typical [1]. We concentrated on the sample containing 2.5 mol% of holmium.

The samples were excited by a 980-nm semiconductor laser (SL, ThorLabs), and the luminescence light, after passing through carefully adjusted optics, was split by a 0.4-m monochromator with a Hamamatsu R928 photomultiplier (PM) at the output. The luminescence light beam was modulated by a mechanical chopper (Terahertz Technologies Inc., model C-995) and, in the detection branch, the signal from the PM was analyzed by a Signal Recovery 7265 lock-in amplifier. In the lifetime measurements, the sample was excited by a pulsed dye laser (OBB-PTI 1012) working at 485 nm with 1-mJ energy in a pulse of 1 ns FWHM. We used a

P. Stremplewski (✉) · C. Koepke · D. Piątkowski
Institute of Physics, Nicolaus Copernicus University, Grudziądzka 5, 87-100 Toruń, Poland
e-mail: patstrem@fizyka.umk.pl

0.4-m prism monochromator and a PM to detect photoluminescence at 540 nm, 652 nm and 766 nm. To collect the signal, a multichannel card with time resolution of 250 ps has been used.

3 Results and discussion

3.1 Emission spectra measurements

Figure 1, being a magnified part of Fig. 2 from [1], illustrates the proposed way of excitation (980 nm). Following predictions made in [1]: that such an excitation would lead to the photon avalanche assisted upconversion, we have ex-
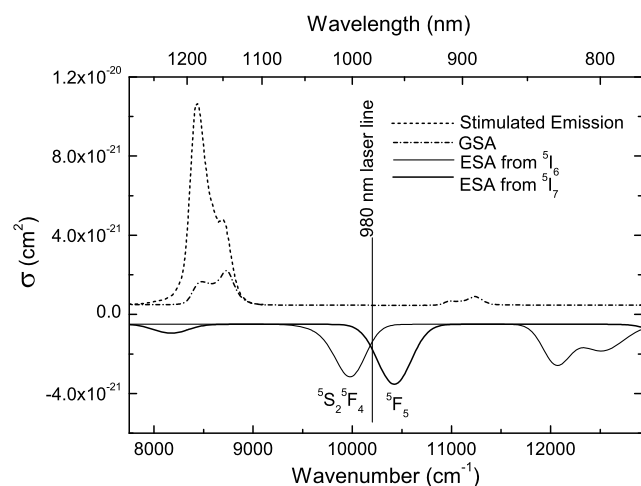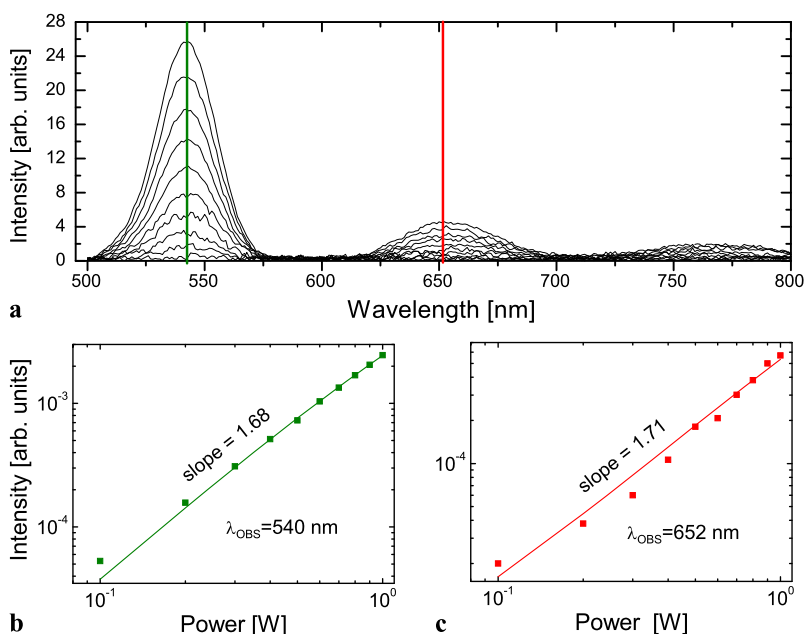

Fig. 1 Situation of the 980-nm excitation with respect to ESA, GSA and stimulated emission peaks

cited almost exactly between two ESA peaks in the region where GSA is practically absent.

Using the excitation source tuned to the line which provides the most efficient sample luminescence (973 nm), the upconverted emission spectra were obtained with power of the SL set from 100 mW up to 1 W with step of 100 mW. Results of the measurements are shown in Fig. 2a. The strongest emission at 540 nm originates in the $^5S_2 {}^5F_4 \rightarrow {}^5I_8$ transition, red emission at 652 nm is due to the $^5F_5 \rightarrow {}^5I_8$ transition and 766-nm luminescence corresponds to the $^5S_2 {}^5F_4 \rightarrow {}^5I_7$ transition. The dependence of the intensity at the peak maximum for 540-nm and 652-nm luminescence on the excitation source power is presented in Fig. 2b and c. Both curves, when following the familiar law $I_{em} \propto P_{ex}^n$ (where n is the number of consecutive exciting photons), are approximately quadratic and could indicate participation of two photons in the upconversion process. However, according to the proposed upconversion mechanism, illustrated on the left-hand side of Fig. 3, there are rather three photons involved in the excitation mechanism: first, a non-resonant photon completed by two lattice phonons, and two photons of the 'pump' ESA transitions starting from $^5I_7$ and $^5I_6$ states. Such a discrepancy with the above formula happens when we deal with some extent of saturation of the system by powerful excitation [12]. This was proved by our calculations (as described in the next subsection) where using weaker and weaker excitation power the $I_{em}(P_{ex})$ function approaches a higher order function. On the other hand, when we theoretically increase the excitation power the parameter n in the $I_{em}(P_{ex})$ function tends to lower values.

We assume that the upconversion is due to the ESA transitions (see Fig. 1): $^5I_7 \rightarrow {}^5F_5$ (center at 960 nm) and

Fig. 2 Upconverted luminescence spectra (**a**), and upconverted luminescence intensity versus excitation power monitored at 540 nm (**b**), monitored at 652 nm (**c**)

Fig. 3 Model of the Ho^{3+} energy levels and the most effective transitions under 973-nm continuous-wave excitation explaining the upconverted emissions from Fig. 2(left) and additional energy transfers compatible with decay profile measurements (right)

$^5I_6 \rightarrow {}^5F_4^5S_2$ (center at 1003 nm). Those transitions explain excitation of the $^5S_2^5F_4$ states but with the assumption that the initial state of the first ESA transition, $^5I_7$, is occupied. Non-zero occupation of this state can be explained by non-resonant ground state absorption $^5I_8 \rightarrow {}^5I_5$ (center at 895 nm). Mismatch between the 973-nm source and the energy of $^5I_5$ is about 1000 cm^{-1} and this can be completed by the energy of two phonons (in ZBLAN, the phonon energy is about 500–600 cm^{-1}) 'borrowed' from the lattice. This energy mismatch makes the GSA process about 250000 less efficient than in the peak of $^5I_8 \rightarrow {}^5I_5$ absorption, but it is still not negligible. However, there is another way to populate the $^5I_7$ state, the following energy transfer: $^5S_2^4F_4$, $^5I_8 \rightarrow {}^5I_4$, $^5I_7$ (see the right-hand side of Fig. 3). To check if our assumptions explain properly the experimental results, we have performed a kinetic simulation of the Ho^{3+} state occupation in the presence of the 973-nm laser source.

3.2 Kinetic analysis and lifetime measurements

To reproduce the upconverted emission characteristics and decay profiles, we should solve the set of rate equations corresponding to the model presented in Fig. 3. The equations are as follows:

$$\frac{dN_{5I8}}{dt} = -\rho_{pump}\frac{\sigma_{GSA}c}{h\nu_{pump}}N_{5I8} + A_{5S2\rightarrow5I8}N_{5S2}$$
$$+ A_{5F5\rightarrow5I8}N_{5F5} - W_{tr2}N_{5I8}N_{5S2},$$

$$\frac{dN_{5I7}}{dt} = -\rho_{pump}\frac{\sigma_{ESA1}c}{h\nu_{pump}}N_{5I7} + w_{5I6}N_{5I6}$$
$$+ A_{5S2\rightarrow5I7}N_{5S2} + W_{tr2}N_{5I8}N_{5S2},$$

$$\frac{dN_{5I6}}{dt} = -\rho_{pump}\frac{\sigma_{ESA2}c}{h\nu_{pump}}N_{5I6} + w_{5I5}N_{5I5} - w_{5I6}N_{5I6},$$

$$\frac{dN_{5I5}}{dt} = \rho_{pump}\frac{\sigma_{GSA}c}{h\nu_{pump}}N_{5I8} + w_{5I4}N_{5I4} - w_{5I5}N_{5I5},$$

$$\frac{dN_{5I4}}{dt} = w_{5F5}N_{5F5} - w_{5I4}N_{5I4} + W_{tr2}N_{5I8}N_{5S2}, \quad (1)$$

$$\frac{dN_{5F5}}{dt} = \rho_{pump}\frac{\sigma_{ESA1}c}{h\nu_{pump}}N_{5I7} + w_{5S2}N_{5S2} - w_{5F5}N_{5F5}$$
$$- A_{5F5\rightarrow5I8}N_{5F5} + W_{tr1}N_{5S2}^2,$$

$$\frac{dN_{5S2}}{dt} = \rho_{pump}\frac{\sigma_{ESA2}c}{h\nu_{pump}}N_{5I6} - A_{5S2\rightarrow5I8}N_{5S2}$$
$$- A_{5S2\rightarrow5I7}N_{5S2} - w_{5S2}N_{5S2}$$
$$- 2W_{tr1}N_{5S2}^2 - W_{tr2}N_{5I8}N_{5S2},$$

$$\frac{dN_{5F3}}{dt} = -w_{5F3}N_{5F3} + W_{tr1}N_{5S2}^2,$$

where N are the state occupations, w are the non-radiative decay rates, A are the radiative decay rates, σ_{pump} is the exciting laser beam energy density, $h\nu_{pump}$ is the excitation source photon energy, σ_{GSA}, σ_{ESA1} and σ_{ESA2} are the ground and excited state absorption cross sections, W_{tr} are the cross-relaxation rates, and c is the speed of light. The states $^5F_3$, $^5F_2$ and $^3K(2)_8$ are treated here jointly and for simplicity denoted as $^5F_3$. Radiative decay rates A are calculated using the Judd–Ofelt theory [1, 13].

To provide the parameters necessary to solve the set (1) and to have better insight into the character of the transitions involved in the whole de-excitation process, we have performed decay profile measurements using a pulsed laser source (485 nm). The excitation, via the ESA, has been addressed to the $^5F_3$, $^5F_2$ and $^3K(2)_8$ states (Fig. 4) and the measured luminescence decays are shown in Fig. 5a–c. Luminescence decays shown in Fig. 5a and b are identical; hence, we can assume that the luminescences at 540 nm and 766 nm occur from the same state. Shapes of these decays suggest a possibility of the energy transfer between Ho^{3+} ions expected in face of high 2.5% mol concentration of dopants in the sample. The luminescence decay profile in

Fig. 4 Model of the Ho³⁺
energy levels and the most
effective transitions under
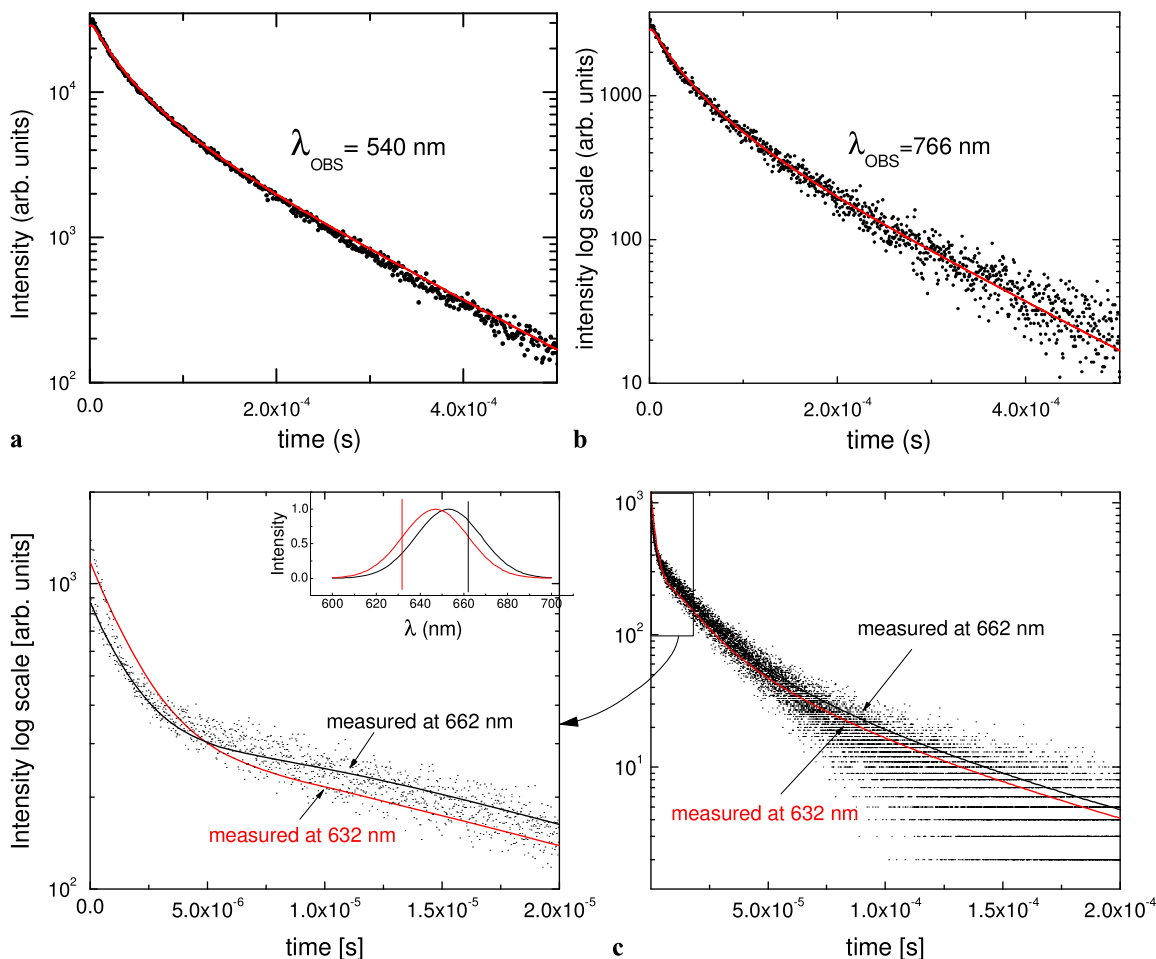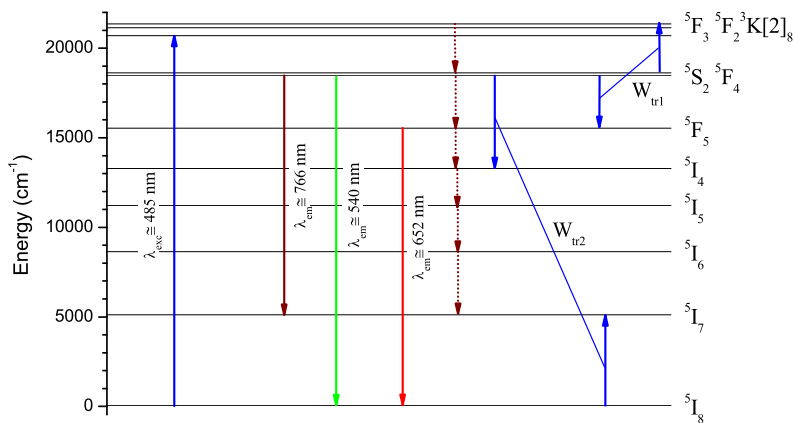485-nm pulse excitation

Fig. 5 Experimental and calculated green (540 nm) (**a**) and infrared (766 nm) (**b**) emission decay. The red emission decay depends on the monitoring line; here we take into account two positions: 632 nm and 662 nm. The experimental points seen in (**c**) are actually two sets of data (taken for 632 and 662 nm) as shown by two separate fits

the presence of energy transfer (of dipole–dipole, donor–acceptor type) is described by the Inokuti–Hirayama formula [14, 15]

$$I(t) = I_0 \exp\left(\frac{-t}{\tau_{RN}} - B\sqrt{\pi \frac{t}{\tau_{RN}}}\right) + C, \qquad (2)$$

where I_0 is an initial luminescence intensity, τ_{RN} is the lifetime (including radiative and non-radiative) in the absence of energy transfer, B is the ratio of acceptor concentration to the critical acceptor concentration and C is a constant value (background noise etc.). We used this formula to find B and
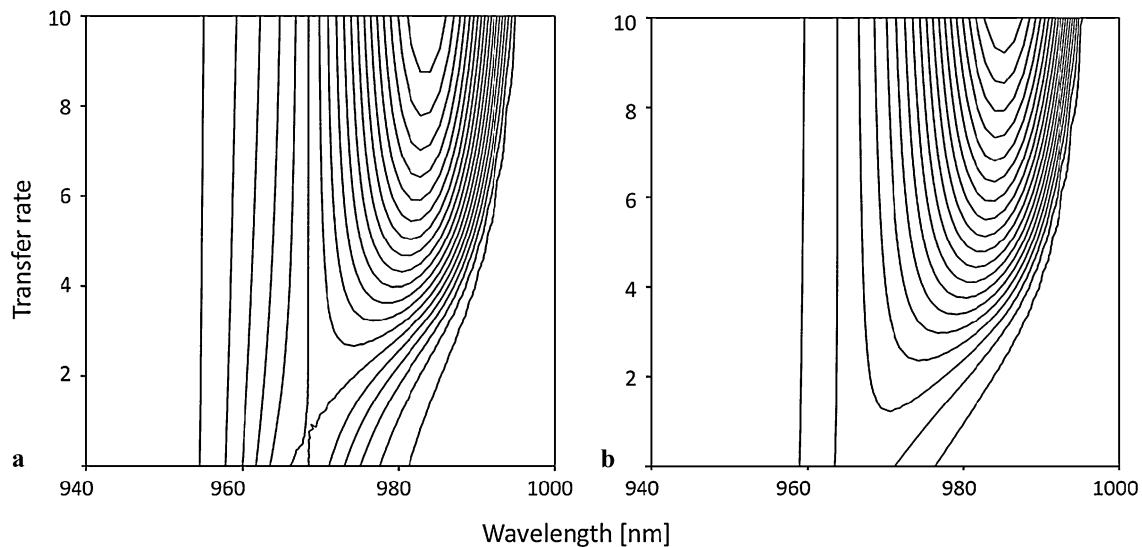
Fig. 6 Calculated contour maps of the upconverted luminescence intensities monitored at: (**a**) 540 nm, (**b**) 650 nm as functions of source wavelength and transfer rate

τ_{RN} as fitting parameters. Calculations suggest that τ_{RN} is about 2.7×10^{-4} s and B is 1.7.

Luminescence decay at ~650 nm (Fig. 5c) seems to be more complicated. We expect that it occurs from the transitions $^5F_3 \rightarrow {}^5I_7$ and $^5F_5 \rightarrow {}^5I_8$. Moreover, it is difficult to measure the $^5F_5$ state lifetime because the occupation of the $^5F_5$ state depends on the $^5S_2$ state lifetime which is much longer, and temporal behavior of the $^5S_2$ state occupation affects the $^5F_5$ state decay at any moment. In the extreme case, if there is no energy transfer from the $^5S_2$ state and no luminescence occurring from the $^5F_3$ state, we should see the $^5F_5$ state decay the same as the $^5S_2$ decay. In this case, we have calculated the $^5F_5$ state decay rate indirectly. In the calculations, we have used a model of Ho³⁺ ion states and the most effective transitions (suitable for the case of 485-nm excitation) as presented in Fig. 4.

To include the results of our lifetime measurements into the kinetic analysis and to find missing coefficients: energy transfer rates and $^5F_5$ state lifetime, we have solved numerically the set (1) substituting different values of W_{tr1}, W_{tr2} and A_{5F5} and comparing results with measured $^5S_2^5F_4$ and $^5F_5$ or $^5F_3$ state decays. We measured luminescence decays at 632 nm and 662 nm and checked if we could reproduce the temporal behavior of the luminescence registered to the left and to the right from the center (see Fig. 5c) and taking into account the luminescence decays from both states calculated with different weights:

$$I(t) \propto N_{5F3}(t) A_{5F3 \rightarrow 5I7} F_{5F3} + N_{5F5}(t) A_{5F5 \rightarrow 5I8} F_{5F5}, \quad (3)$$

where F_{5F3} and F_{5F5} are the weights of the transitions indicated in Fig. 4, $N_{5F3}(t)$ and, $N_{5F5}(t)$ are the calculated time-dependent occupations of upper states and A are the radiative transition rates.

The best fit of the relation (3) to the experimental results gives $W_{tr1} = 800$ s⁻¹, $W_{tr2} = 200$ s⁻¹, $w_{5F3} \cong 5 \times 10^5$ s⁻¹ and $w_{5F5} \cong 1.7 \times 10^5$ s⁻¹. These values have been used in kinetic analysis by means of solving the rate equations (1). The numerical calculations were performed with use of the fourth-order Runge–Kutta routine.

Results of calculations are presented in the form of solid lines fitting the experimental data in Fig. 2b and c and in Fig. 5a–c.

4 Conclusions

We have proved that it is possible to obtain upconverted emissions in the ZBLAN:Ho³⁺ glass with non-resonant excitation at ~980 nm. We have performed kinetic analysis supported by additional lifetime measurements and proposed a model explaining the observed characteristics. It appears that the photon avalanche effect is not necessary to obtain the upconverted emissions, as predicted in [1]; the upconversion is via the ESA transitions in the frame of a single ion, although the energy transfer plays an important role in feeding some states and in decay profiles.

Moreover, using this model and substituting source wavelength and energy transfer rates as variables, it is possible to calculate contour maps of the excitation spectra versus concentration of the Ho³⁺ ions (expressed as a transfer rate). The result of these calculations is shown in Fig. 6. Let us assume that the transfer rate unit is the value corresponding to the case of 2.5% Ho³⁺ concentration in the ZBLAN glass. To obtain the contour maps, both transfer rates ($W_{tr1} = 800$ and $W_{tr2} = 200$) were multiplied by the factor labeled on the vertical axes and, with the assumption that the transfer rate is
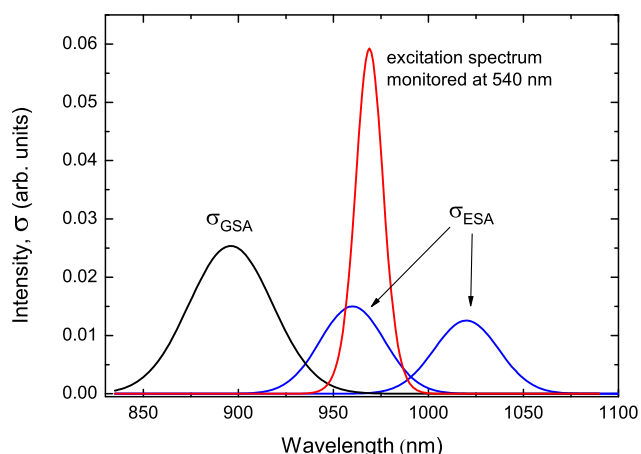
Fig. 7 Calculated excitation spectrum of the ZBLAN sample with 2.5% Ho^{3+} concentration, and its position in relation to the GSA and ESA spectra

proportional to the concentration, we obtained contour maps of excitation spectra as a function of Ho^{3+} concentration (here the intensity axis is perpendicular to the figure plane). It is seen that a distinct shift towards longer waves can be expected due to the rising concentration of holmium ions. Understanding of this shift can be more clear when looking at the calculated excitation spectrum for 2.5% Ho^{3+} expected at 540 nm (Fig. 7). When the transfer rate is small or does not occur, the main contribution to the first excited state population is the ground state absorption. In this case, we should have a relatively large overlap between the GSA spectrum and excitation source spectrum; hence, we expect the maximum of the excitation spectrum at about 960 nm. The energy transfer, when it becomes more efficient, takes over the main role in the $^5I_7$ state feeding. When the energy transfer is the main process which populates the $^5I_7$ state and since it is proportional to the second power of the $^5S_2^5F_4$ state occupation, the crucial factor populating the $^5S_2^5F_4$ state is the ESA transitions. Then the maximum of the excitation peak shifts toward longer waves. The calculated spectrum agrees very well with experiment. The excitation source wavelength was set by the SL temperature in the range 966 nm to 982 nm, and then the luminescence monitored at 540 nm had a sharp maximum at 973-nm laser wavelength.

The further challenge is the experimental verification of the excitation spectrum changes with the change of concentration of Ho^{3+} ions. Unfortunately, currently available are only ZBLAN glass samples with lower concentrations of holmium ions in which the mentioned effects do not occur. Luminescence decay measurements in the samples

of lower concentration of Ho^{3+} can provide only obvious information about the transfer rate decrease with the decrease of the concentration of ions. Such results do not give any information about the shift of the excitation spectrum maximum towards longer waves, expected in the samples of much bigger (more than 2.5 mol%) ion concentration.

References

1. D. Piątkowski, K. Wiśniewski, M. Różański, Cz. Koepke, M. Kaczkan, M. Klimczak, R. Piramidowicz, M. Malinowski, J. Phys., Condens. Matter **20**, 155201 (2008)
2. M. Malinowski, A. Wnuk, Z. Frukacz, G. Chadeyron, R. Mahiou, S. Guy, M.-F. Joubert, J. Alloys Compd. **323–324**, 731 (2001)
3. A. Wnuk, M. Kaczkan, R. Piramidowicz, R. Mahiou, G. Bertrand, M.-F. Joubert, M. Malinowski, Radiat. Eff. Defects Solids **158**, 469 (2003)
4. M. Kowalska, G. Klocek, R. Piramidowicz, M. Malinowski, J. Alloys Compd. **380**, 156 (2004)
5. A.F.H. Librantz, S.D. Jackson, F.H. Jagosich, L. Gomes, G. Poirier, S.J.L. Ribeiro, Y. Messaddeq, J. Appl. Phys. **101**, 123111 (2007)
6. T. Sumiyoshi, H. Sekita, T. Arai, S. Sato, M. Ishihara, M. Kikuchi, IEEE J. Sel. Top. Quantum Electron. **5**, 936 (1999)
7. M.-F. Joubert, Opt. Mater. **11**, 181 (1999)
8. F. Auzel, Phys. Rev. B **13**, 2809 (1976)
9. Cz. Koepke, D. Piątkowski, K. Wiśniewski, M. Naftaly, J. Non-Cryst. Solids **356**, 435 (2010)
10. A.S. Gouveia-Neto, E.B. da Costa, L.A. Bueno, S.J.L. Ribeiro, J. Lumin. **110**, 79 (2004)
11. J.C. Boyer, F. Vetrone, J.A. Capobianco, A. Speghini, M. Bettinelli, Chem. Phys. Lett. **390**, 403 (2004)
12. M. Pollnau, D.R. Gamelin, S.R. Lüthi, H.U. Güdel, M.P. Hehlen, Phys. Rev. B **61**, 3337 (2000)
13. D. Piątkowski, K. Wiśniewski, C. Koepke, R. Piramidowicz, M. Klimczak, M. Malinowski, Appl. Phys. B **93**, 809 (2008)
14. B. Henderson, G.F. Imbusch, *Optical Spectroscopy of Inorganic Solids* (Clarendon Press, Oxford, 1989)
15. R.C. Powell, *Physics of Solid-State Laser Materials* (American Institute of Physics, New York, 1998)